Epitaxial Relationship for Hexagonal-to-Cubic Phase Transition in a Block Copolymer Mixture

Mark F. Schulz and Frank S. Bates*
Department of Chemical Engineering and Materials Science, University of Minnesota, Minneapolis, Minnesota 55455

Kristoffer Almdal and Kell Mortensen
Risø National Laboratory, Roskilde, Denmark
(Received 2 February 1994)

Small-angle neutron scattering experiments have revealed an epitaxial relationship between the hexagonal cylinder phase, and a bicontinuous cubic phase with $Ia\bar{3}d$ space group symmetry, in a poly(styrene)-poly(2-vinylpyridine) diblock copolymer mixture. Proximity to the order-disorder transition and an inelastic low frequency rheological response suggest that the cubic phase is stabilized by fluctuations. These results identify block copolymers as model compounds for investigating the thermodynamics and dynamics of complex "soft" condensed matter.

PACS numbers: 61.12.Ex, 61.50.Jr, 64.70.Kb, 81.30.Hd

Order-order phase transitions in condensed matter provide one of the most important mechanisms for manipulating and optimizing material properties. Nucleation and growth of new phases frequently occur with preferred crystallographic orientations that are governed by symmetry and lattice spacing relationships between the original and transformed states. Such epitaxial growth has been characterized and exploited in many solid-state compounds that exhibit short-range (i.e., atomic scale) order. However, our understanding of order in "soft" materials, characterized by short-range disorder, is more primitive, and the epitaxial relationships between different ordered phases have only recently been considered [1,2]. In this Letter we identify the epitaxy between hexagonally packed cylinders and a bicontinuous cubic phase ($Ia\bar{3}d$ space group) for a diblock copolymer melt. To the best of our knowledge this phase transition has not been reported previously in block copolymers, although it is known to occur in solvated surfactant systems [1–4]. Our results suggest that block copolymers represent a valuable tool for exploring the structure and properties of soft condensed matter.

Block copolymers are amphiphilic molecules that belong to a broad class of compounds that can assemble into ordered phases, composed of periodic microstructures that are locally disordered and fluidlike. Surfactants, such as membrane-forming lipids [3,4], certain thermotropic liquid crystals [5], and some colloids [6], are included in this category of materials. A combination of factors make block copolymers particularly attractive for studying the fundamental thermodynamic and dynamic aspects of soft matter. The composition, overall molecular size, and polymer block types can be varied, and precisely controlled, through well established synthetic procedures, leading to a variety of ordered microstructures [7]. Recently, we have discovered a rich polymorphism near the order-disorder transition (ODT) that mimics the phase behavior of certain liquid crystal systems [8,9]. One of the order-order phase transitions, hexagonal- (cylinders) to-cubic (bicontinuous with $Ia\bar{3}d$ space group) is particularly intriguing since it involves the most commonly encountered lyotropic cubic phase [3,4]. Surprisingly, only very recently (here and Ref. [10]) has this phase been identified in block copolymers.

Results reported here were obtained from a poly(styrene)-poly(2-vinylpyridine) (PS-PVP) diblock copolymer mixture where the overall PS volume fraction was $\langle f \rangle = 0.37$. The two components in the mixture were $f = 0.35$ and $f = 0.40$ diblocks with $N = 200$ and polydispersity index $N_w/N_n = 1.05$, where N is the degree of polymerization. Deuterated PS blocks provided excellent neutron scattering contrast. In the unmixed state the $f = 0.35$ and 0.40 polymers assemble into hexagonal and lamellar phases that disorder at $T_{ODT} = 207\,^{\circ}C$ and $232\,^{\circ}C$, respectively. By mixing these two compounds we have been able to map the complex phase behavior of the PS-PVP system between the hexagonal and lamellar phases. In a separate report [11] we will show that these mixed diblock specimens, characterized by relatively small degrees of size (N) and compositional (f) heterogeneity, can be treated as pseudosingle component systems, i.e., they exhibit the same phase behavior and epitaxy as pure diblocks. The mixed specimen was prepared by dissolution in tetrahydrofuran followed by precipitation and drying under vacuum.

Small-angle neutron scattering (SANS) experiments were used to characterize the ordered states in the PS-PVP block copolymer. Measurements were conducted at the National Institute of Standards and Technology (NIST) on the NIST/Exxon/University of Minnesota 30 m instrument using $\lambda = 5.5$ Å wavelength neutrons ($\Delta\lambda/\lambda = 0.14$) and a sample-to-detector distance of 3.4 m. Structural analysis was facilitated by aligning the low temperature phase using a dynamic shearing device described elsewhere [12,13]. All SANS experiments

0031-9007/94/73(1)/86(4)$06.00

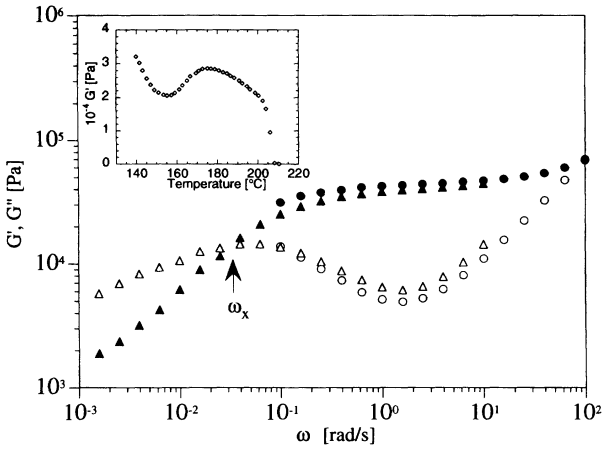

FIG. 1. Dynamic mechanical elastic (G') (○, △) and loss (G'') (○, △) shear moduli as a function of frequency at 175 °C (○, ○) and 200 °C (△, △) . These data have been superimposed via a horizontal shift of the 175 °C results [14]. Crossover from a solid to inelastic response at ω_x is attributed to fluctuation effects in the cubic phase. The inset shows isochronal ($\omega = 0.5$ rad/s) measurements obtained while heating the PS-PVP specimen at 1 °C/min. Order-order and order-disorder transitions are evidenced by the increase and decrease in G' at approximately 150 °C and 205 °C, respectively.

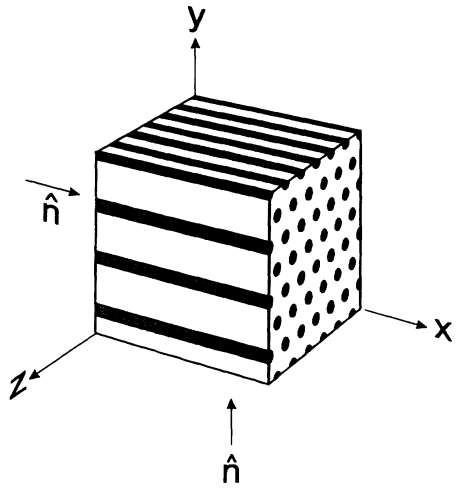

FIG. 2. Monodomain structure of low temperature shear-aligned hexagonal cylinder phase. Shear direction is x while the plane of shear x-z is parallel to the (10) hexagonal plane. SANS experiments reported here were obtained with the neutron beam ($\hat{\mathbf{n}}$) directed along the x and y axes.

reported here were conducted after the shear field was turned off and a well-annealed state had been achieved. By quenching the material below the glass transition temperature ($T_g \cong 100$ °C for PS and PVP), the high temperature phases could be frozen and then examined with arbitrary neutron beam orientation; during *in situ* SANS experiments the neutron beam can only be directed normal to the plane of shear [12].

Isochronal dynamic elastic (G') and loss (G'') modulus measurements indicate order-order and order-disorder phase transitions at 150 °C and 205 °C, respectively (see inset in Fig. 1). Isothermal measurements, following a jump from 140 °C to 175 °C, show that the order-order transition is completed in roughly 1 h. SANS experiments conducted on the shear-aligned material at 140 °C identify the hexagonal cylinder morphology illustrated in Fig. 2. Intensity contour plots obtained with the neutron beam directed parallel to the cylinder axis (i.e., in the $\mathbf{q}_y$-$\mathbf{q}_z$ scattering plane), presented in Fig. 3(a), display hexagonal symmetry with at least 3 orders of reflections at q^*, $\sqrt{3}q^*$, $\sqrt{4}q^*$ where $q^* = 2\pi/d_{10}$ with $d_{10} = 170$ Å; $q = |\mathbf{q}| = 4\pi\lambda^{-1}\sin(\theta/2)$ is the magnitude of the scattering wave vector. Weak diffuse reflections are found in $\mathbf{q}_x$-$\mathbf{q}_z$ consistent with this assignment. (Here we note that the $|\mathbf{q}_z| = \sqrt{3}q^*$ reflection is relatively weak in $\mathbf{q}_x$-$\mathbf{q}_z$ due to a coincident extinction in the cylindrical form factor.) Strong reflections at $|\mathbf{q}_y| = q^*$ and $\sqrt{4}q^*$ are also found in $\mathbf{q}_x$-$\mathbf{q}_y$ (not shown). This shear-induced orientation is identical to that reported earlier for a PEP-PEE diblock copolymer melt [14].

Upon heating, both the viscoelastic properties and structural symmetry change dramatically. The frequency dependence of G' and G'' at 175 °C and 200 °C, in the high temperature phase, are illustrated in Fig. 1; these results have been superimposed by a horizontal shift [14]. Over a wide range of frequencies the material behaves like a solid ($G' \sim \omega^0$), but crosses over to an inelastic response ($G' < G''$) below a certain characteristic frequency, ω_x. We will comment further in this interesting spectrum below.

SANS and small-angle x-ray scattering (SAXS) experiments, and transmission electron microscopy (TEM) performed on a variety of polycrystalline and oriented PS-PVP specimens, and several other diblock copolymer melts, have led us to conclude that the high temperature phase contains the same cubic ($Ia\bar{3}d$ space group) bicontinuous morphology originally identified by Luzzati and Spegt [15], and now found in many lipid-water systems [1–4]. Hajduk *et al.* [10] have also recently identified this phase in a PS-PI diblock copolymer based on SAXS powder diffraction and TEM experiments. A complete description of our analysis will be provided elsewhere [9, 11]. Powder [11] and monodomain (see below) diffraction patterns identify the leading order cubic reflections as {211} and {220}; this condition is unique to the $Ia\bar{3}d$ and $I\bar{4}3d$ space groups. TEM analysis reveals threefold and fourfold projections that mimic simulated images of the bicontinuous microstructure [10], favoring the $Ia\bar{3}d$ symmetry. Moreover, we are unaware of any bicontinuous morphology with $I\bar{4}3d$ symmetry.

In characterizing the structural changes associated with the order-order transition we focus on $\mathbf{q}_x$-$\mathbf{q}_z$ and $\mathbf{q}_y$-$\mathbf{q}_z$ scattering patterns taken after heating the oriented

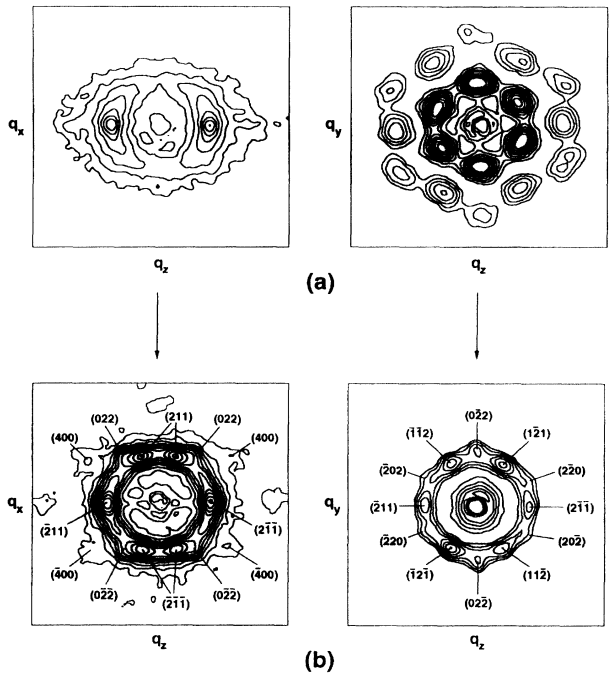

FIG. 3. (a) SANS intensity contour plots taken at 140 °C, from the shear-aligned hexagonal cylinder phase (see Fig. 2). (b) Intensity contour plots obtained at 175 °C after heating oriented samples from 140 °C. The reflections have been indexed based on the $Ia\bar{3}d$ space group and the epitaxy shown in Fig. 4. Duplicate reflections derive from a 180 °C rotation about the [111] direction. All contour levels depict logarithmic variations in intensity in half-decade increments.

hexagonal state from 140 °C to 175 °C. Intensity contour plots obtained at 175 °C are presented in Fig. 3(b). The most intense peaks in the high temperature phase, at $q^* = 0.035$ Å^{-1}, correspond to the family of first-order {211} reflections. The phase transition has placed the [111] direction (threefold axis) of the cubic unit cell along the original sixfold hexagonal (i.e., cylinder) axis. If we associate the $|\mathbf{q}_z| = q^*$ peaks in Fig. 3(b) with $(\bar{2}11)$ and $(2\bar{1}\bar{1})$ reflections, then the additional q^* scattering peaks at azimuthal angles of $\pm 60°$ in $\mathbf{q}_y$-$\mathbf{q}_z$ correspond to $(11\bar{2})$, $(1\bar{2}1)$, $(\bar{1}\bar{1}2)$, and $(\bar{1}2\bar{1})$, respectively. This assignment anticipates two pairs of q^* reflections in $\mathbf{q}_x$-$\mathbf{q}_z$ at azimuthal angles of $\pm 90°$, 19.5°, and $-160.5°$ relative to $\mathbf{q}_x$ (i.e., [111]): $(2\bar{1}\bar{1})$, $(\bar{2}11)$ and (211), $(\bar{2}\bar{1}\bar{1})$. A third pair of q^* reflections in $\mathbf{q}_y$-$\mathbf{q}_z$ at $-19.5°$ and $+160.5°$ are obtained by a 180° rotation of the unit cell about the [111] axis. Because these two unit cell orientations are degenerate under the hexagonal-to-cubic epitaxy (see below) equal populations will be produced in a macroscopic specimen. This is confirmed by the $\mathbf{q}_x$-$\mathbf{q}_z$ scattering pattern; note that the $|\mathbf{q}_z| = q^*$ reflections are roughly twice as intense as the other four as anticipated by this mechanism.

Higher order reflections are also seen in both scattering patterns. In $\mathbf{q}_y$-$\mathbf{q}_z$ $(02\bar{2})$ and $(0\bar{2}2)$ diffraction peaks are plainly evident, rotated 30° from $(11\bar{2})$ and $(\bar{1}\bar{1}2)$. Four other $\{2\bar{2}0\}$ reflections are also present, although these are considerably weaker. As we have demonstrated elsewhere [14], shear alignment produces the strongest correlations between (10) planes of cylinders that are parallel to the plane of shear (this is the x-z plane in Fig. 2). Consequently, heating from the oriented hexagonal phase produces stronger correlations along $\mathbf{q}_y$ in the cubic structure which results in the enhanced intensity in $(02\bar{2})$ and $(0\bar{2}2)$. Because the $\mathbf{q}_x$-$\mathbf{q}_z$ scattering plane is accessed with the sample precisely aligned in the shearing device, this beam orientation provides the most balanced SANS patterns, and one additional set of higher order of reflections. In the $Ia\bar{3}d$ space group, the {211} and {220} reflections are followed by {321} and {400} [3]. With our orientation, only (400) and $(\bar{4}00)$ reflections will be projected onto $\mathbf{q}_x$-$\mathbf{q}_z$ and indeed these are seen, as identified in Fig. 3(b).

The microstructure that we associate with the cubic phase consists of two independent interpenetrating networks composed of "rods" joined by trifunctional connectors [3, 4, 15]. A schematic projection of this bicontinuous morphology along the [111] direction is presented in Fig. 4, together with the associated hexagonal cylinder structure, yielding the following epitaxial relationship : (10) $\longleftrightarrow$ $(0\bar{2}2)$ and (11) $\longleftrightarrow$ $(1\bar{2}1)$. This result is quite appealing as it coordinates the sixfold hexagonal and threefold cubic symmetry elements with the exact lattice matching condition: $2d_{11}/d_{10} = d_{1\bar{2}1}/d_{2\bar{2}0} = \sqrt{8}/\sqrt{6}$. In a related work Clerc, Levelut, and Sadoc [2] have reported a different expitaxial relationship, (10) $\longleftrightarrow$ (211),

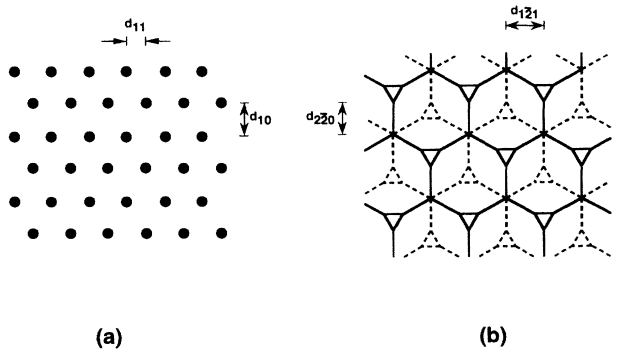

FIG. 4. Epitaxial relationship between the hexagonal cylinder and bicontinuous $Ia\bar{3}d$ phases. Projections are along the cylinder axis (a), and [111] direction of the cubic unit cell (b). Solid and dashed curves signify two independent three-dimensional networks constructed from threefold connectors [2–4]. Solid and dashed triangular elements correspond the right- and left-handed helices. The SANS results depicted in Fig. 3 indicate an epitaxy based on the correspondence (10) $\longleftrightarrow$ $(2\bar{2}0)$ and (11) $\longleftrightarrow$ $(1\bar{2}1)$. This relationship transforms the sixfold hexagonal axis to a threefold cubic one while preserving the ratio of lattice spacings: $2d_{11}/d_{10} = d_{1\bar{2}1}/d_{2\bar{2}0} = \sqrt{8}/\sqrt{6}$.

for surfactant water systems. TEM images of an actual coherent epitaxial surface captured during the hexagonal-to-cubic transition in a PS-PI specimen will be presented elsewhere [9].

Transformation of the cylindrical microstructure to the bicontinuous one converts a parabolic dividing surface (e.g., that associated with the inflection point in the local composition field) characterized by zero Gauss curvature, into a hyperbolic one with negative Gauss curvature [4]. This type of topological change and the exact nature of the dividing surface have received much attention in recent years in efforts to explain the complex structure and properties of certain lyotropic liquid crystalline systems [16]. We have not yet extended our analysis to an interpretation of the actual transformation mechanism. Nevertheless, these results demonstrate that block copolymers provide a uniquely attractive class of materials for characterizing the thermodynamic behavior of such complex soft matter.

We conclude with a few remarks about the dynamical properties of the bicontinuouis cubic phase (Fig. 1). Permanent networks (e.g., gels) are characterized by a frequency independent elastic modulus, $G' \sim \omega^0$. The rheological response found in Fig. 2 resembles that of a temporary network, such as an entangled polymer melt [17], which is characterized by a molecular relaxation time $\tau \sim \omega_x^{-1}$; for $\omega \ll \omega_x$ polymer melts behave like liquids ($G' \sim \omega^2$, $G'' \sim \omega^1$). However, the low frequency ($\omega < \omega_x$) behavior for the bicontinuous structure is clearly not liquidlike. Instead, it resembles what we have recently associated with creeping deformation in bcc (spherical microstructure) diblock copolymer melts near the ODT [13]. This suggests that near the disordering transition the bicontinuous cubic phase is fluctuating, and that sufficiently slow deformations can be accommodated by locally breaking and reforming the structure. Similar arguments have been used to rationalize the rheological properties of wormlike micellar systems that display viscoelastic responses that are remarkably similar to that shown in Fig. 1 [18]. This hypothesis is further supported by a paucity of higher order reflections, and our observation [11] that the $\mathbf{q}_x$-$\mathbf{q}_z$ scattering pattern is unaffected by large strain, low frequency shearing. Moreover, this biontinuous phase appears to be localized near the order-disorder transition [9–11], which has been shown to be fluctuation induced [14, 19]. These facts indicate that fluctuations may play a key role in stabilizing the bcc state, as anticipated theoretically by Brazovskii and coworkers [20].

Support for this research was provided by the U.S. Air Force Office of Scientific Research (AF/F49620-93) and the Center for Interfacial Engineering, a National Science Foundation Engineering Research Center at the University of Minnesota.

*To whom correspondence should be addressed.

[1] Y. Rancon and J. Charvolin, J. Phys. Chem. **92**, 2646 (1988).
[2] M. Clerc, A.M. Levelut, and J.F. Sadoc, J. Phys. II (France) **1**, 1263 (1991).
[3] P. Mariani, V. Luzzati, and H. Delacroix, J. Mol. Biology **204**, 165 (1988).
[4] J.M. Seddon, Biochim. Biophys. Acta **1031**, 1 (1990).
[5] P.S. Pershan, *Structure of Liquid Crystal Phases* (World Scientific, Teoneck, NJ, 1988).
[6] L.D. Chen, C.F. Zukoski, B.J. Ackerson, H.J.M. Hanley, G.C. Straty, J. Barker, and C.J. Glinka, Phys. Rev. Lett. **69**, 688 (1992).
[7] F.S. Bates and G.H. Fredrickson, Annu. Rev. Phys. Chem. **41**, 525 (1990).
[8] I.W. Hamley, K.A. Koppi, J.H. Rosedale, F.S. Bates, K. Almdal, and K. Mortensen, Macromolecules **26**, 5959 (1993).
[9] S. Förster, A. Khandpur, J. Zhao, F.S. Bates, I.W. Hamley, A.T. Ryan, and W. Bras (to be published).
[10] D.A. Hajduk, P.E. Harper, S.M. Gruner, C.C. Honeker, G. Kim, E.L. Thomas, and L.J. Fetters (to be published).
[11] M.F. Schulz, F.S. Bates, D.A. Hajduk, and S.M. Gruner (to be published).
[12] K.A. Koppi, M. Tirrell, and F.S. Bates, Phys. Rev. Lett. **70**, 1449 (1993).
[13] K.A. Koppi, M. Tirrell, F.S. Bates, K. Almdal, and K. Mortensen, J. Rheol. (to be published).
[14] K. Almdal, F.S. Bates, and K. Mortensen, J. Chem. Phys. **96**, 9122 (1992).
[15] V. Luzzati and P.A. Spegt, Nature (London) **215**, 701 (1967).
[16] S.T. Hyde, J. Phys. (Paris), Colloq. **7**, C-209 (1990).
[17] P.-G. deGennes, *Scaling Concepts in Polymer Physics* (Cornell University Press, Ithaca, NY, 1979).
[18] T.M. Clausen, P.K. Vinson, J.R. Minter, H.T. Davis, Y. Talmon, and W.G. Miller, J. Phys. Chem. **96**, 474 (1992).
[19] F.S. Bates, J.H. Rosedale, G.H. Fredrickson, and C.J. Glinka, Phys. Rev. Lett. **61**, 2229 (1988); K.A. Koppi, M. Tirrell, and F.S. Bates, *ibid.* **70**, 1449 (1993).
[20] S.A. Brazovskii, Zh. Eksp. Teor. Fiz. **68**, 175 (1975) [Sov. Phys. JETP **41**, 88 (1975)]; S.A. Brazovskii, I.E. Dzyaloshinskii, and A.R. Moratov, *ibid.* **93**, 1110 (1987) [**66**, 625 (1987)].

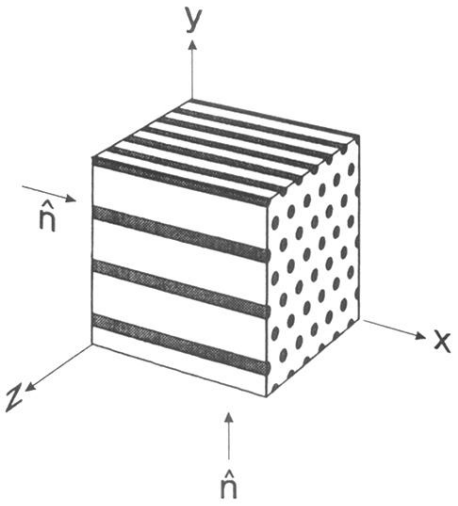

FIG. 2. Monodomain structure of low temperature shear-aligned hexagonal cylinder phase. Shear direction is x while the plane of shear x-z is parallel to the (10) hexagonal plane. SANS experiments reported here were obtained with the neutron beam ($\hat{\mathbf{n}}$) directed along the x and y axes.

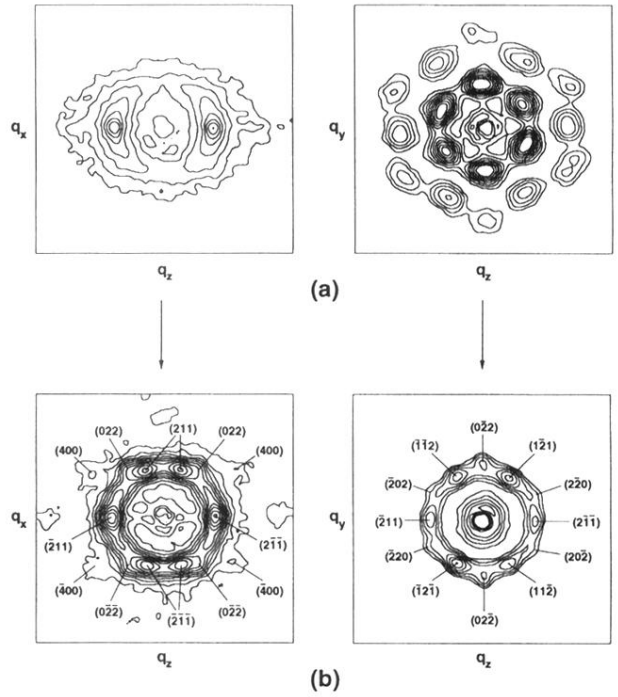

FIG. 3. (a) SANS intensity contour plots taken at 140 °C, from the shear-aligned hexagonal cylinder phase (see Fig. 2). (b) Intensity contour plots obtained at 175 °C after heating oriented samples from 140 °C. The reflections have been indexed based on the $Ia\bar{3}d$ space group and the epitaxy shown in Fig. 4. Duplicate reflections derive from a 180 °C rotation about the [111] direction. All contour levels depict logarithmic variations in intensity in half-decade increments.